JAAS

ROYAL SOCIETY OF CHEMISTRY

TECHNICAL NOTE

View Article Online
View Journal | View Issue

Cite this: *J. Anal. At. Spectrom.*, 2020, **35**, 238

Rapid determination of the original boron isotopic composition from altered basaltic glass by *in situ* secondary ion mass spectrometry†

Miaohong He, *[a] Xiaoping Xia, [a] Xiaolong Huang,[a] Jinlong Ma, [a] Jieqiong Zou,[ab] Qing Yang,[a] Fan Yang,[a] Yanqiang Zhang,[a] Yanan Yang[a] and Gangjian Wei [a]

The determination of the original boron (B) isotopic composition in altered basaltic glass is important to characterize magma generation and evolution in the mantle. Traditional whole-rock analysis of the B isotopic composition of basaltic glass requires time-consuming pretreatment for removing the altered section. Here, a protocol of *in situ* B isotopic analysis of basaltic glass by secondary ion mass spectrometry was developed using an accessible reference material BCR-2G which was first ascertained as a standard material for *in situ* B-isotopic analysis, whose B isotopic value ($\delta^{11}B = -5.44‰$; $2\sigma = 0.55‰$) was determined by solution-based multi-collector-inductively coupled plasma-mass spectrometry in this study. Trans-sectional analysis of both slightly and extensively altered grains was performed from the cores outward to the rims (palagonite) by this *in situ* method to verify its ability in rapidly extracting information of the original (unaltered) B composition from natural samples. The $\delta^{11}B$ values of the pristine (unaltered) melt ranging from −8.99‰ to −12.00‰ could be rapidly determined from the slightly altered grain, which is distinguishable from those of its transition (−3.14‰ to +9.56‰) and palagonite (+5.04‰ to +8.56‰) sections. Compared with the slightly altered one, the extensively altered grain has just the transition and palagonite sections without the pristine section. Therefore, *in situ* B isotopic profiling analysis of basaltic glass is beneficial for rapidly obtaining original magma B information from a single natural altered grain.

Received 31st October 2019
Accepted 5th December 2019

DOI: 10.1039/c9ja00374f

rsc.li/jaas

1. Introduction

Basaltic glass is a product of the rapid chilling of magma with low susceptibility to crystallization fractionation[1] and is commonly found in submarine, subglacial, and lacustrine environments.[2] Boron (B) is a highly fluid-mobile element with markedly different concentrations and isotopic compositions in seawater (4.5 ppm; $\delta^{11}B = +39.5‰$), mantle (<1 ppm; $\delta^{11}B = -8‰$ to $-12‰$), and continental crust (2–28 ppm; $\delta^{11}B = -10.5‰$).[3–6] B isotopic analysis of basaltic glass is therefore widely considered as a direct and efficient tool for characterizing the evolution of mantle magma through processes such as slab subduction and the interactions within ocean–crust–mantle systems.[4,7–9] However, the thermodynamic instability of basaltic glass means that it is susceptible to alteration in the presence of an aqueous phase, with such an alteration commencing very soon after the eruption of basaltic magma.[1,10] In studies of magma evolution and related fields, it is necessary to distinguish the pristine section from the naturally altered sample, which is easily achieved based on their distinct optical and structural features if the alteration part is the secondary phase (palagonite).[10,11] However, the interior of a glass chip away from palagonite or the slightly altered glass without significant secondary phases may lead to uncertainty as to whether the B isotopic composition of the chip represents pristine glass, as must be determined to accurately establish both the source and evolution of the formation magma.

Traditional whole-rock analytical methods involving thermal ionization mass spectrometry (TIMS) and multi-collector-inductively coupled plasma-mass spectrometry (MC-ICP-MS)[4,6,12,13] are known for their excellent precision in B isotopic analyses but have difficulty in rapidly and completely resolving unaltered and altered materials.[14] It is therefore important to develop a method for *in situ* B isotopic microanalysis of basaltic glass. Laser-ablation MC-ICP-MS and secondary ion mass spectrometry (SIMS) are the two most common *in situ* methods.[5,9,15–21] The former method has been reported to be able to determine B isotopic compositions of glass with very low B contents with a laser in scan mode, but the background and

[a]*State Key Laboratory of Isotope Geochemistry, Guangzhou Institute of Geochemistry, Chinese Academy of Sciences, Guangzhou 510640, China. E-mail: mhhe@gig.ac.cn; Fax: +86-20-85290130; Tel: +86-20-85290501*

[b]*Beijing No. 12 High School, 100071, China*

† Electronic supplementary information (ESI) available. See DOI: 10.1039/c9ja00374f

destruction of the sample surface are problematic.[22] Ultra-high vacuum (10^{-9} to 10^{-10} torr) SIMS with highly useful ion yield permits more precise analyses on a microscale and wider application than, for example, LA-ICP-MS.[5,8,18,23] SIMS is thus the optimal option for *in situ* analysis of low-B basaltic glass. More importantly, compared with whole-rock analysis methods which produce average compositions of fresh and altered parts of glass or rock, such *in situ* methods offer a rapid route to determine the original B isotopic composition from natural glass.

For this study, *in situ* B isotopic analysis of basaltic glass by SIMS was developed with a well-known but newly established *in situ* B isotopic analysis reference material, BCR-2G, which is better matched to natural basaltic glass with respect to the B content and matrix composition as well as more easily accessible compared with that used in previous SIMS analyses. Other reference materials GSD-1G, BHVO-2G, BIR-1G, GOR128-G, GOR132-G and StHs6/80-G were used to evaluate the feasibility of the method. The unknown B isotopic compositions of BCR-2G, BHVO-2G and BIR-1G were also determined by solution-based MC-ICP-MS. Two naturally altered submarine basaltic glasses were analyzed, along the grain cores towards (palagonite) the rims to evaluate the capacity of the method to rapidly ascertain the pristine (unaltered) B isotopic compositions from a single natural grain.

2. Materials and methods

2.1 SIMS

SIMS boron isotopic composition and elemental content analyses were conducted using a CAMECA IMS 1280-HR ion microprobe at the State Key Laboratory of Isotope Geochemistry, Guangzhou Institute of Geochemistry, Chinese Academy of Science (SKLaBIG-CAS), Guangzhou, China. The instrumental parameters were as follows: the primary $^{16}O^-$ ion-beam current was 100 nA and 40 nA with a voltage of 13 kV, the secondary acceleration voltage was 10 kV, ± 50 eV energy-window without offset, and a 60 μm × 60 μm raster was applied during pre-sputtering for 240 s to remove the gold layer and reduce surface contamination. Gaussian illumination was adopted to ensure a high transmission of ions from the raster area through the 4 mm × 4 mm field aperture and exclude the edge of the secondary beam and thereby reduce the influence of surface contamination.[24] Secondary ion detection involved the use of a single electron multiplier in counting mode with a raster area of 30 μm × 30 μm (actual sampling area of ~50 μm × 55 μm) in the center of a larger pre-sputtered area (60 μm × 60 μm). There were 40 cycles per analysis, with each cycle involving 20 s and 10 s counting time for $^{10}B^+$ and $^{11}B^+$, respectively. The mass resolution ($M/\Delta M$) was set to 1500 at 10% intensity, which was sufficient to resolve potential interferences of $^1H^9Be^+$ and $^1H^{10}B^+$ with $^{10}B^+$ and $^{11}B^+$, respectively.

2.2 Sample descriptions and analytical procedures

Two basaltic glasses samples were collected from a deep basin (>2500 m depth) in the South China Sea at site U1434 during the International Ocean Discovery Program Expedition 349 in 2014, as described by Li, *et al.*[25,26] The samples comprise mid-ocean-ridge basalt (MORB) glass with palagonite formed at *ca.* 12 Ma.[25–27] The brown rims (palagonite) of black basaltic glass (Fig. 1) resulted from low-temperature alteration.[23] The samples were separated into slightly (Fig. 1a) and extensively (Fig. 1b) altered basaltic glass, based on the thickness of palagonite and visible glass porosity.[10,11] Profile analyses were conducted from the core of basaltic glass outwards to the palagonite, with analysis spot locations being recorded in microscope images (Fig. 1e and f), which were the photographs of the altered samples after the experiment with their gold coatings having been removed.

Reference materials used in this study include four US Geological Survey basaltic glasses BCR-2G (B content = 6.2 ± 1.1 ppm),[28] BHVO-2G (B = 5.5 ± 1.31 ppm),[28] BIR-1G (B = 1.6 ± 0.67 ppm) and GSD-1G (B = 48 ± 20 ppm; $\delta^{11}B$ = +10.1‰ ± 1.0‰),[29,30] two MPI-DING komatiite glasses (GOR128-G (B = 23.5 ± 2.8 ppm; $\delta^{11}B$ = +13.55 ± 0.21‰) and GOR132-G (B = 17.2 ± 2.6 ppm; $\delta^{11}B$ = +7.11 ± 0.97‰),[18,31,32] and one MPI-DING dacite glass StHs6/80-G (B = 11.8 ± 1.3 ppm; $\delta^{11}B$ = −4.48‰ ± 0.29‰)[18,31,32]). National Institute of Standards and Technology (NIST) reference materials of the SRM61 series, with well-established B contents and isotopic homogeneity,[15] were not used due to differences between their matrix and basaltic glass,

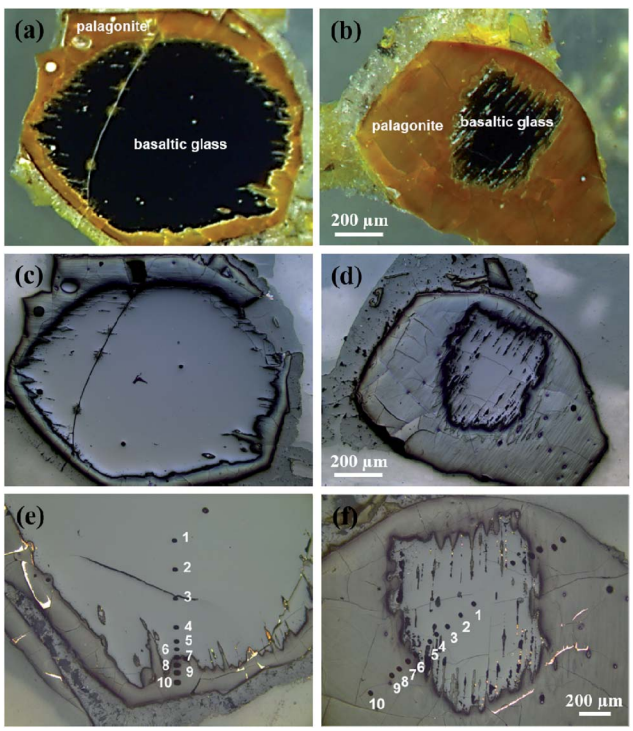

Fig. 1 Transmitted-light (a and b) and reflected-light (c and d) microscope images of the altered basaltic glass samples showing brown palagonite alteration rims. Images (a) and (c) are of a slightly altered grain, and (b) and (d) are of an extensively altered grain. (e) and (f) are the microscope images of the section of the slightly and extensively altered glass after the experiment with its gold coatings removed, where the black circles are the analysis spots.

which reduces the accuracy of SIMS analyses.[17] Although this effect can be effectively suppressed with the assistance of a high voltage offset,[17] it is impractical for the natural basaltic glass with a very low B content. As for the analysis of palagonite, it is difficult to define and characterize suitable reference materials nowadays because of their heterogeneous composition containing smectites, clays, oxides and so on.[10,11,33–35] SIMS B isotopic analyses of palagonite were therefore corrected by whole-rock palagonite analysis by MC-ICP-MS.

All analyzed glass samples were large fragments of 0.6–2.5 mm in diameter, which were mounted in epoxy resin and polished to a flat and even surface. Thorough cleaning before analysis involved repeated ultrasonic cleaning with high-purity ethanol and boron-free water.[24,36] Analysis spots were located at least 100 μm from the glass edges to avoid potential contamination from the interface between the sample and resin.

The seven reference materials were analyzed before the samples, where the $\delta^{11}B$ values of materials BCR-2G, BHVO-2G and BIR-1G were also determined by conventional MC-ICP-MS because of the lack of their reported $\delta^{11}B$ values, following the procedures of Wei *et al.*[37] with an analysis sequence background–SRM951–background–sample–background–SRM951 and a geological standard rock reference BCR-2 (4.2 ppm; $\delta^{11}B = -5.9 \pm 0.2‰$)[37] being used as their monitoring standard. Two natural basaltic glasses were analyzed to check the application of our SIMS method in rapidly determining the original (unaltered) B isotopic composition from naturally altered glass, which is performed under a high primary beam current (100 nA). The B isotopic compositions relative to NIST SRM 951 ($^{11}B/^{10}B_{SRM951} = 4.04362$) were calculated as follows:[14,16,38]

$$\delta^{11}B_m = (({}^{11}B/{}^{10}B_m)/({}^{11}B/{}^{10}B_{SRM951}) - 1) \times 1000 \quad (1)$$

$$\delta^{11}B_{corrected} = \delta^{11}B_m - IMF \quad (2)$$

where $^{11}B/^{10}B_m$ and $\delta^{11}B_m$ are the raw isotopic ratio ($^{11}B/^{10}B$) and the raw B isotopic value of the sample measured by SIMS, respectively. The SIMS instrumental mass fractionation (IMF) defines the difference between the measured B isotopic value by SIMS and that from MC-ICP-MS with respect to the reference material BCR-2G.

The determination of the relationship between the B content and its isotopic composition during alteration requires the simultaneous measurement of B contents of the altered sample during isotopic analysis, which is impossible to achieve with traditional methods using $^{30}Si^+$ or $^{28}Si^{2+}$ as a reference ion because they would have to be analyzed separately.[17,24] Here, B contents were determined directly, based on calibrations by standards with respect to their $^{11}B^+$ signal measured simultaneously during the B isotopic analysis.

3. Results and discussion

3.1 Comparison of boron isotopic analysis of silicate glass by SIMS under primary beam currents of 40 nA and 100 nA

The SIMS *in situ* B isotopic analysis method normally employs a primary beam current of 20–40 nA,[15,18,39] which extends to 100 nA while performing the analysis of the low B content sample;[16,23] however, a detailed study on a high primary beam current has been seldom reported, which motivates the comparison of the effect of primary beam currents of 40 and 100 nA on the B isotopic analysis herein to act as a potential guidance for future analyses of low B samples.

The effect of both primary beam currents (100 and 40 nA) on the measurement repeatability of individual B isotope determinations is displayed in Fig. 2. This figure indicates that the precision of analyses of materials was correlated with the boron content and the primary beam current, the extent of which especially enlarges for the low B content glass. Additionally, the ion count rates and the $^{11}B/^{10}B$ ratio were monitored during each analysis (Fig. 3). The slopes of the linear regression of the $^{11}B/^{10}B$ ratio over forty cycles (experimental setting conditions) were almost not significantly different from zero within the standard error and no systematic drift of ion count rates and isotope ratios occurred under the two primary beam currents (Fig. 3a and b), which indicates that the crater and charging effect could be ruled out. However, these effects would appear with sputter times longer than sixty cycles, as can be seen in Fig. 3c and d. The B count rates significantly decreased and the ratios of $^{11}B/^{10}B$ were widely dispersed after 60 analytical cycles under a primary beam current of 100 nA (Fig. 3c), which is different from that of 40 nA under which the B count rates increased with the analytical cycles (Fig. 3d). This phenomenon can be explained from the fact that stronger material sputtering results from the deviation of the focus of the primary ion beam with increasing analytical cycles within a certain depth, which would then enlarge the sampling area; therefore, the amount of secondary ions (^{10}B and ^{11}B) could be found to increase (Fig. 3d). However, the higher primary ion beam current (100 nA) producing much larger crater depth, derived from the stronger sputtering rate, and greater charge effect compared with that of the lower primary ion beam current result in restraining the extraction of B ions from the bottom of sampling crater, which can be seen from Fig. 3c where B counts rates

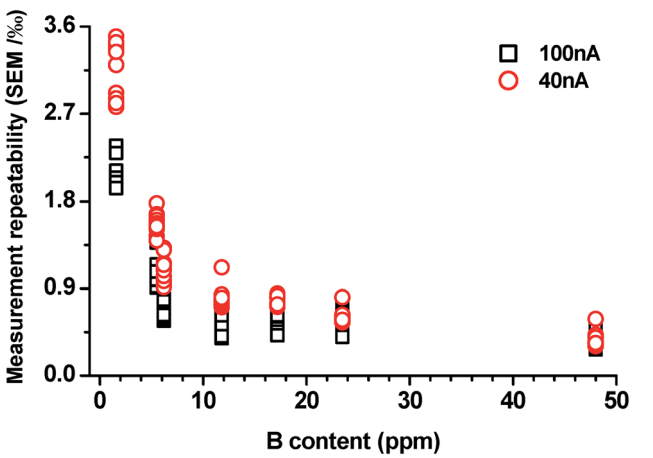

Fig. 2 Measurement repeatability of individual B isotope determination for reference materials. Two primary beam currents of 100 and 40 nA were used.

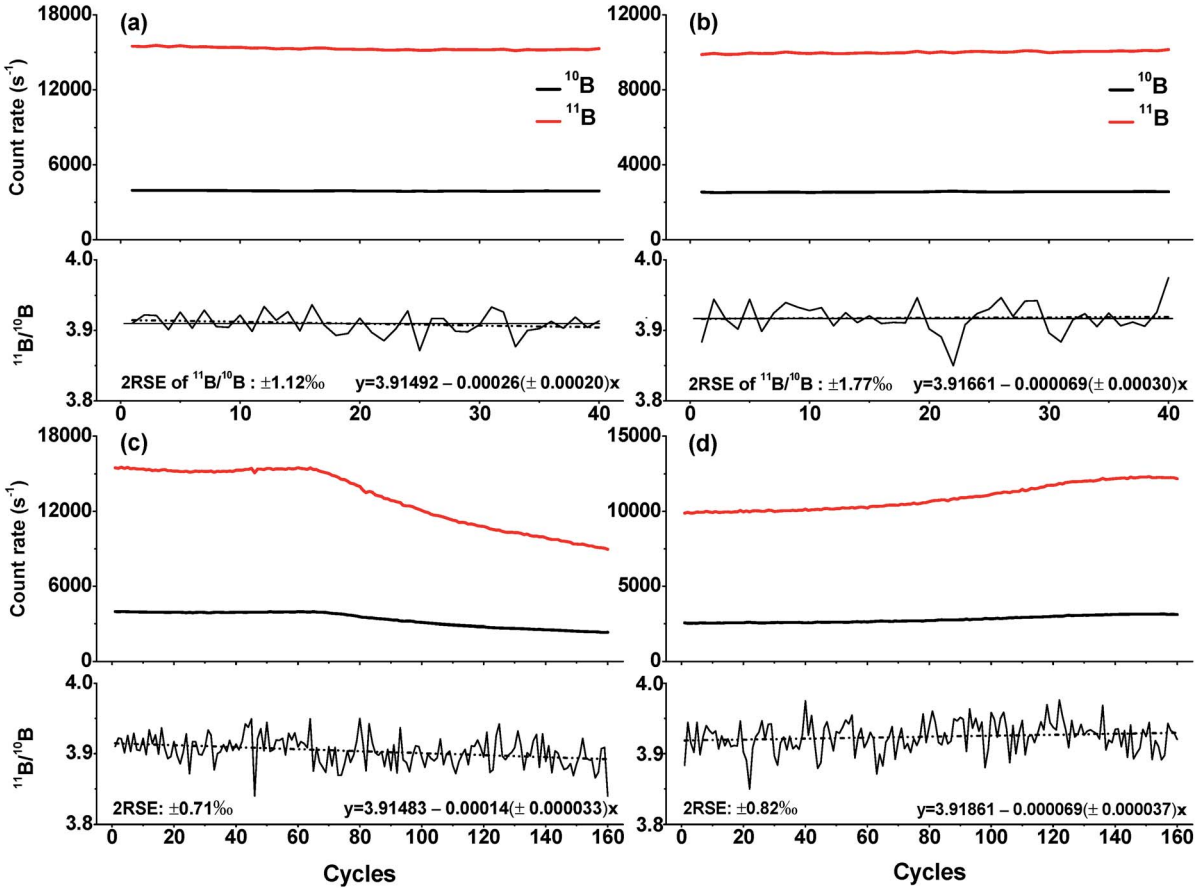

Fig. 3 Typical ^{11}B and ^{10}B signals and ^{11}B/^{10}B ratios of the reference material BCR-2G over (a) a 40-cycle analysis with a primary beam current of 100 nA; (b) a 40-cycle analysis with a primary beam current of 40 nA; (c) a 160-cycle analysis with a primary beam current of 100 nA and (d) a 160-cycle analysis with a primary beam current of 40 nA. RSE is the relative error for 40 cycles of ^{11}B/^{10}B in (a) and (b) and for 160 cycles in (c) and (d), respectively.

significantly decreased with longer sputter times. Briefly, 40 analytical cycles would be suitable and reasonable considering the analytical results as well as the cost.

The B isotopic analysis result of the reference material BCR-2G is exhibited in Fig. 4, which shows good reproducibility of random spot analyses of different fragments in different

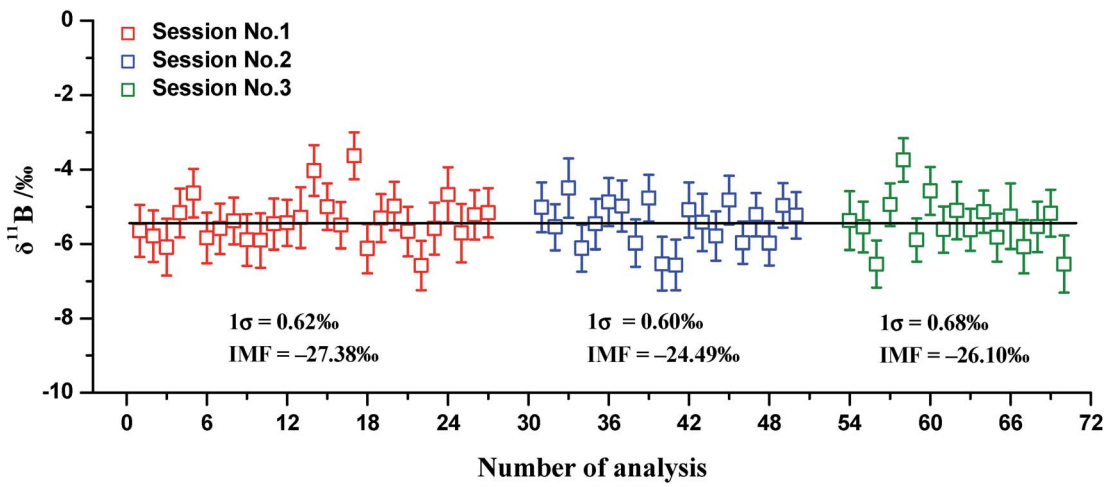

Fig. 4 Reproducibility of the δ^{11}B value of different BCR-2G fragments measured by SIMS in different sessions (error bars correspond to the internal precision for a single spot measurement). 1σ represents the standard deviation for all measurements in each session and IMF is the mean instrumental mass fractional for each session. The primary beam current was 100 nA.

analysis sessions. This material, BCR-2G, therefore, could be used as a new standard of *in situ* SIMS B isotopic analysis due to its homogenous B isotopic composition. The other six reference materials, BIR-1G, BHVO-2G, GSD-1G, GOR128-G, StHs6/80-G and GOR132-G, were used to evaluate the feasibility and accuracy of the method based on the new B isotopic calibration standard, BCR-2G. Their δ^{11}B values and external reproducibility, measured by SIMS under both two primary beam current settings, are given in Table 1, with the results being consistent with those obtained by other methods. Moreover, the external reproducibility for the low B reference materials is better under the higher primary beam current. Therefore, for the B isotopic analysis of the low B sample by SIMS, the higher primary beam current would be a superior option.

3.2 Boron isotopic and elemental composition analyses of altered basaltic glass

The glass/palagonite interface is always distinct and sharp (Fig. 1c and d), but laser microscope thickness analysis confirmed the difference of their thicknesses was about 4.6 μm (Fig. 5), whose effect on SIMS analysis should be insignificant. The interface occupies a zone ~100 μm thick covered with microchannels entering the fresh glass. Variations in the B isotopic composition of the slightly altered basaltic glasses, from the core of the grain out towards the palagonite rim, are shown in Fig. 6a. Three distinct sections can be distinguished: (1) pristine glass (spots 1–4) with uniform δ^{11}B values (−8.99‰ to −12.00‰; 2σ = 2.6‰) within the range of the primitive mantle (−10‰ ± 2‰),[40] and possibly reflecting the original magmatic composition directly inherited from the mantle without contamination; (2) a transition layer (spots 5–6) where δ^{11}B values increase from −3.14‰ to +9.56‰; and (3) palagonite, with δ^{11}B values ranging from +5.04‰ (2SE = ± 0.66) to +8.56‰ (2SE = ± 1.46), which have been corrected by its IMF (−28.60‰), defined as the difference between the average all SIMS measurements and the MC–ICPMS value (δ^{11}B = +5.75‰ ± 1.36‰, N = 3). In the extensively altered glass (Fig. 6b), two distinct sections are evident, including the transition layer where δ^{11}B values increase from −6.92‰ in the core to +9.30‰ at the interface between the glass and palagonite and the palagonite layer with values ranging from +3.22‰ to +6.85‰. In Fig. 6b there is no a section representing pristine glass, which suggests that the core of this grain has also been modified.

Similar to the B isotopic trend, the B content of the pristine glass section, which is calibrated by the reference materials according to Fig. 7, is almost constantly 2.08 ppm over spots 1–4 in the slightly altered glass, decreasing to 1.06 ppm (spots 5–6) near the interface between glass and palagonite (Fig. 6c), while the B content of the extensively altered glass (Fig. 6d) decreases steadily from the initial value of 2.01 ppm in the core to

Table 1 Comparison of the δ^{11}B values of reference materials measured by SIMS and other methods[a]

			Measured by SIMS							
			I_{prim} = 100 nA			I_{prim} = 40 nA			Measured by other methods	
Name	Composition	[B] (μg g^{-1})	δ^{11}B (‰)	2SD (‰)	N	δ^{11}B (‰)	2SD (‰)	N	δ^{11}B (‰)	Reference or this study
BCR-2G	Basaltic	6.2	−5.44	1.12	28	−5.44	1.64	15	−5.44 ± 0.55	MC-ICPMS (this study)
BIR-1G	Basaltic	1.6	−4.1	2.63	15	−5.03	4.7	15	−1.13 ± 0.99	MC-ICPMS (this study)
BHVO-2G	Basaltic	5.5	−4.07	1.89	15	−5.03	2.6	15	−1.82 ± 0.96	MC-ICPMS (this study)
GSD-1G	Basaltic	48	+8.98	1.95	15	+9.72	1.58	15	+10.1 ± 1.0	TIMS (Jochum *et al.*, 2011)[29]
StHs6/80-G	Dacite	11.8	−5.71	1.63	15	−5.85	1.75	15	−4.48 ± 0.29	TIMS (Rosner and Meixner, 2010)[31]
GOR 132-G	Komatiite	17.2	+7.29	2.54	15	+5.85	1.54	15	+7.11 ± 0.97	TIMS (Rosner and Meixner, 2010)[31]
GOR 128-G	Komatiite	23.5	+12.86	2.8	15	+12.88	1.68	15	+13.55 ± 0.21	TIMS (Rosner and Meixner, 2010)[31]

[a] The instrumental mass fractionation (IMF) of SIMS was determined based on the reference material BCR-2G, where IMF = $\delta^{11}B_{m\ (SIMS)} - \delta^{11}B_{m\ (MC\text{-}ICPMS)}$ = −32.82‰ − (−5.44‰) = −27.38‰ in terms of I_{prim} = 100 nA, and IMF = −26.53‰ for I_{prim} = 40 nA.

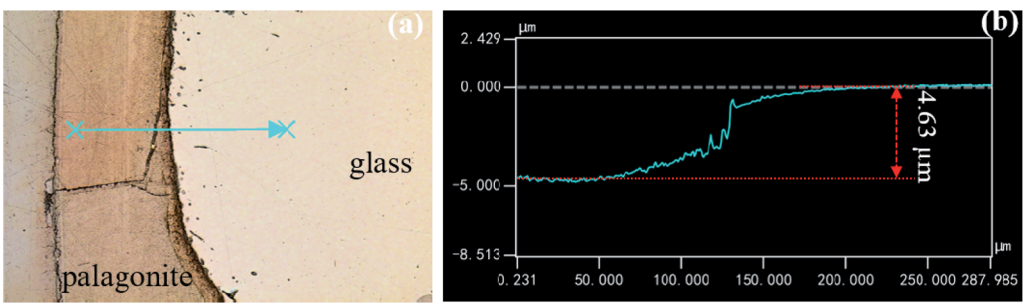

Fig. 5 Thickness analysis of altered basaltic glass in the epoxy resin using a laser microscope (Keyence VK-X250); (a) the raw shape of palagonite and glass; (b) thickness profile analysis according to the blue line in (a).

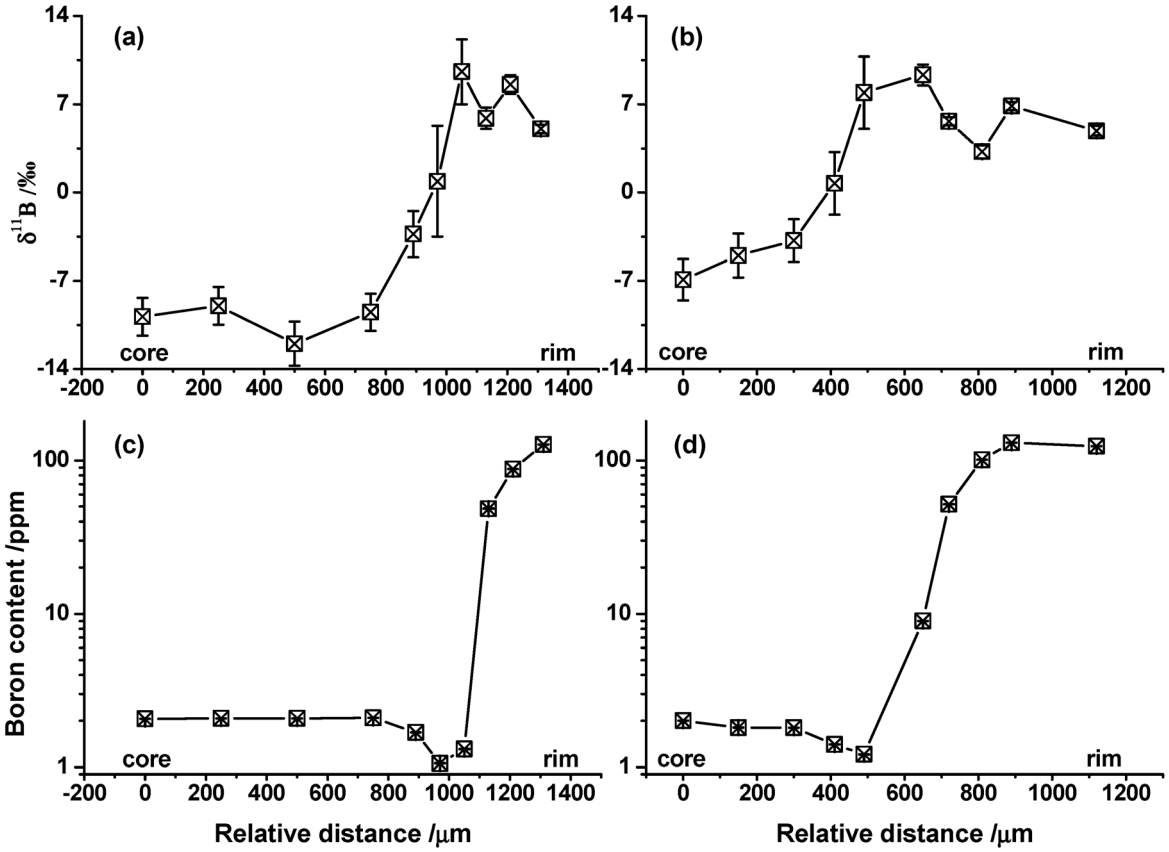

Fig. 6 Boron isotopic profiles of (a) slightly and (b) extensively altered glass, and their corresponding boron content profiles are shown in (c) and (d) respectively. Both boron isotopic composition and content were determined by SIMS simultaneously (analysis-spot locations as in Fig. 1e and f). The distance is relative to the core of the grain, and error bars represent 1σ.

1.21 ppm at the interface. A combination of δ^{11}B and B content trends within the transition layers indicates either solid leaching, where ^{10}B was preferentially leached relative to ^{11}B,[41–43] or SIMS sampling mixing the glass and some invisible dissolved or re-precipitated materials from the alteration event.[10,33,43]

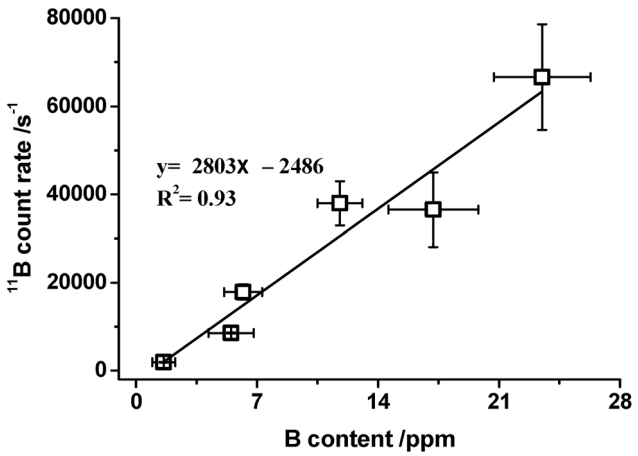

Fig. 7 The calibration curve of $^{11}B^+$ counts *vs.* the boron content of the six reference materials, BIR-1G, BHVO-2G, BCR-2G, StHs6/80-G, GOR132-G, and GOR128-G.

The transition layer of basaltic glass has δ^{11}B values of −6.92‰ to about +9.56‰, quite different from those of pristine glass ($\delta^{11}B = -8.99$‰ to −12.00‰), but its appearance is almost identical to the pristine section. In earlier studies, either extra acid leaching or abrasion under microscopic examination was used to remove the alteration section from natural glass,[4,7,44,45] although the mineralogical similarity of altered transition and pristine sections makes such a removal difficult. The determination of the original B composition from the altered sample may therefore be a significant factor in determining the mantle magma B isotopic heterogeneity or the degree of contamination of magma by seawater, oceanic crust, or melt from subducted crust. *In situ* B profiling thus provides a more rapid and accurate method of distinguishing pristine and altered sections of natural basaltic glass than those used previously.

The δ^{11}B value systematically decreases from +9.56‰ at the interface between palagonite and basaltic glass to +3.22‰ to +8.56‰ within palagonite (Fig. 6a and b). The total B content increases from about 1.2 ppm at the interface to a value of more than 120 ppm at the rim (Fig. 6c and d). Such a large range of values of δ^{11}B and B contents might be caused by varying degrees of palagonitization. In the early stages of palagonitization, the interface between glass and palagonite, where the glass is directly exposed to seawater, has high δ^{11}B values consistent with B uptake from a high-δ^{11}B source such as seawater ($\delta^{11}B =$

+39.5‰).[4,10,11] However, at depth within the palagonite, the total B content is gradually increased to ~27 times that of seawater (4.5 ppm), consistent with previous observation that oceanic basalts altering to secondary phases can incorporate considerable B into their crystal structures at low–moderate temperatures.[46] However, the large varying range of B isotopic composition of palagonite could be due to heterogeneity and multiple phases in the palagonite;[10,11] in addition, the coexistence of tetrahedral and exchangeable B sites within palagonite with noticeably different isotopic compositions could also be responsible.[33,34]

4. Conclusions

In situ SIMS B isotopic analyses were developed by SIMS based on a newly established B isotopic reference material, BCR-2G. Two submarine basaltic glasses with different extents of alteration were used to evaluate the method. Three distinct sections—pristine glass, transition and palagonite—were identified within a single grain, indicating the ability of SIMS to rapidly and conveniently provide B isotopic information for original mantle-derived melt from altered natural glasses based on profiling analysis from the grain core towards the rim, which may help in future application in the study of magma evolution, alteration of oceanic crust and the oceanic B cycle.

Conflicts of interest

There are no conflicts to declare.

Acknowledgements

The authors would like to thank Professor Klaus Peter Jochum for providing the MPI-DING reference materials. The English of the manuscript was improved by Stallard Scientific Editing. This work was supported by the National Natural Science Foundation of China (41803010), the GIGCAS 135 Project (135PY201605), the Guangzhou Institute of Geochemistry (TGC201804) and the State Key Laboratory of Isotope Geochemistry (Grants SKLaBIG-QD-18-01 and SKLaBIG-JY-19-04).

References

1 S. Dultz, J. Boy, C. Dupont, M. Halisch, H. Behrens, A.-M. Welsch, M. Erdmann, S. Cramm, G. Helsch and J. Deubener, *Geomicrobiol. J.*, 2014, **31**, 813–834.
2 B. Parruzot, P. Jollivet, D. Rébiscoul and S. Gin, *Geochim. Cosmochim. Acta*, 2015, **154**, 28–48.
3 I. H. Thorseth, H. Furnes and O. Tumyr, *Geochim. Cosmochim. Acta*, 1991, **55**, 731–749.
4 S. Krolikowska-Ciaglo, A. Deyhle, F. Hauff and K. Hoernle, *Chem. Geol.*, 2007, **242**, 455–469.
5 H. R. Marschall, V. D. Wanless, N. Shimizu, P. A. E. Pogge von Strandmann, T. Elliott and B. D. Monteleone, *Geochim. Cosmochim. Acta*, 2017, **207**, 102–138.
6 K.-D. Zhao, S.-Y. Jiang, E. Nakamura, T. Moriguti, M. R. Palmer, S.-Y. Yang, B.-Z. Dai and Y.-H. Jiang, *Ore Geol. Rev.*, 2011, **43**, 243–248.
7 M. Chaussidon and A. Jambon, *Earth Planet. Sci. Lett.*, 1994, **121**, 277–291.
8 M. Brounce, M. Feineman, P. LaFemina and A. Gurenko, *Geochim. Cosmochim. Acta*, 2012, **94**, 164–180.
9 A. A. Gurenko and V. S. Kamenetsky, *Earth Planet. Sci. Lett.*, 2011, **312**, 201–212.
10 N. A. Stroncik and H.-U. Schmincke, *Int. J. Earth Sci.*, 2002, **91**, 680–697.
11 N. A. Stroncik and H. U. Schmincke, *Geochem., Geophys., Geosyst.*, 2001, **2**, DOI: 10.1029/2000gc000102.
12 H. Marschall and G. Foster, *Boron Isotopes: The Fifth Element*, Springer, 2017.
13 M. R. Palmer and J. F. Slack, *Contrib. Mineral. Petrol.*, 1989, **103**, 434–451.
14 L. H. Chan and F. A. Frey, *Geochem., Geophys., Geosyst.*, 2003, **4**, DOI: 10.1029/2002gc000365.
15 S. Kasemann, A. Meixner, A. Rocholl, T. Vennemann, M. Rosner, A. K. Schmitt and M. Wiedenbeck, *Geostand. Newsl.*, 2001, **25**, 405–416.
16 M. Chaussidon, F. Robert, D. Mangin, P. Hanon and E. F. Rose, *Geostand. Newsl.*, 1997, **21**, 7–17.
17 A. Gurenko, I. Veksler, A. Meixner, R. Thomas, A. Dorfman and D. Dingwell, *Chem. Geol.*, 2005, **222**, 268–280.
18 H. R. Marschall and B. D. Monteleone, *Geostand. Geoanal. Res.*, 2015, **39**, 31–46.
19 Q. L. Li, X. H. Li, Y. Liu, F. Y. Wu, J. H. Yang and R. H. Mitchell, *Chem. Geol.*, 2010, **269**, 396–405.
20 Y. Liu, Q. L. Li, G. Q. Tang, X. H. Li and Q. Z. Yin, *J. Anal. At. Spectrom.*, 2015, **30**, 979–985.
21 A. A. Gurenko, R. B. Trumbull, R. Thomas and J. M. Lindsay, *J. Petrol.*, 2005, **46**, 2495–2526.
22 P. J. le Roux, S. B. Shirey, L. Benton, E. H. Hauri and T. D. Mock, *Chem. Geol.*, 2004, **203**, 123–138.
23 A. A. Gurenko and M. Chaussidon, *Chem. Geol.*, 1997, **135**, 21–34.
24 H. Marschall and T. Ludwig, *Mineral. Petrol.*, 2004, **81**, 265–278.
25 C.-F. Li, X. Xu, J. Lin, Z. Sun, J. Zhu, Y. Yao, X. Zhao, Q. Liu, D. K. Kulhanek, J. Wang, T. Song, J. Zhao, N. Qiu, Y. Guan, Z. Zhou, T. Williams, R. Bao, A. Briais, E. A. Brown, Y. Chen, P. D. Clift, F. S. Colwell, K. A. Dadd, W. Ding, I. H. Almeida, X.-L. Huang, S. Hyun, T. Jiang, A. A. P. Koppers, Q. Li, C. Liu, Z. Liu, R. H. Nagai, A. Peleo-Alampay, X. Su, M. L. G. Tejada, H. S. Trinh, Y.-C. Yeh, C. Zhang, F. Zhang and G.-L. Zhang, *Geochem., Geophys., Geosyst.*, 2014, **15**, 4958–4983.
26 C.-F. Li, J. Lin, D. Kulhanek, T. Williams, R. Bao, A. Briais, E. Brown, Y. Chen, P. Clift and F. Colwell, *Expedition 349 Summary*, 2015.
27 A. A. P. Koppers, *On the $^{40}Ar/^{39}Ar$ dating of low-potassium ocean crust basalt from IODP Expedition 349, South China Sea*, AGU, San Francisco, USA, 15–19 Dec, 2014.
28 Z. C. Hu, Y. S. Liu, M. Li, S. Gao and L. S. Zhao, *Geostand. Geoanal. Res.*, 2009, **33**, 319–335.

29 K. P. Jochum, S. A. Wilson, W. Abouchami, M. Amini, J. Chmeleff, A. Eisenhauer, E. Hegner, L. M. Iaccheri, B. Kieffer, J. Krause, W. F. McDonough, R. Mertz-Kraus, I. Raczek, R. L. Rudnick, D. Scholz, G. Steinhoefel, B. Stoll, A. Stracke, S. Tonarini, D. Weis, U. Weis and J. D. Woodhead, *Geostand. Geoanal. Res.*, 2011, **35**, 193–226.
30 K. P. Jochum, M. Willbold, I. Raczek, B. Stoll and K. Herwig, *Geostand. Geoanal. Res.*, 2005, **29**, 285–302.
31 M. Rosner and A. Meixner, *Geostand. Geoanal. Res.*, 2010, **28**, 431–441.
32 K. P. Jochum, B. Stoll, K. Herwig, M. Willbold, A. W. Hofmann, M. Amini, S. Aarburg, W. Abouchami, E. Hellebrand, B. Mocek, I. Raczek, A. Stracke, O. Alard, C. Bouman, S. Becker, M. Dücking, H. Brätz, R. Klemd, D. de Bruin, D. Canil, D. Cornell, C.-J. de Hoog, C. Dalpé, L. Danyushevsky, A. Eisenhauer, Y. Gao, J. E. Snow, N. Groschopf, D. Günther, C. Latkoczy, M. Guillong, E. H. Hauri, H. E. Höfer, Y. Lahaye, K. Horz, D. E. Jacob, S. A. Kasemann, A. J. R. Kent, T. Ludwig, T. Zack, P. R. D. Mason, A. Meixner, M. Rosner, K. Misawa, B. P. Nash, J. Pfänder, W. R. Premo, W. D. Sun, M. Tiepolo, R. Vannucci, T. Vennemann, D. Wayne and J. D. Woodhead, *Geochem., Geophys., Geosyst.*, 2006, **7**, DOI: 10.1029/2005gc001060.
33 A. Drief and P. Schiffman, *Clays Clay Miner.*, 2004, **52**, 622–634.
34 B. D. Pauly, L. B. Williams, R. L. Hervig, P. Schiffman and R. A. Zierenberg, *Clays Clay Miner.*, 2014, **62**, 224–234.
35 J. L. Crovisier, J. Honnorez and J. P. Eberhart, *Geochim. Cosmochim. Acta*, 1987, **51**, 2977–2990.
36 D. M. Shaw, M. D. Higgins, M. G. Truscott and T. A. Middleton, *Am. Mineral.*, 1988, **73**, 894–900.
37 G. Wei, J. Wei, Y. Liu, T. Ke, Z. Ren, J. Ma and Y. Xu, *J. Anal. At. Spectrom.*, 2013, **28**, 606–612.
38 L. B. Williams, R. L. Hervig, J. R. Holloway and I. Hutcheon, *Geochim. Cosmochim. Acta*, 2001, **65**, 1769–1782.
39 K. Kobayashi, R. Tanaka, T. Moriguti, K. Shimizu and E. Nakamura, *Chem. Geol.*, 2004, **212**, 143–161.
40 M. Chaussidon and B. Marty, *Science*, 1995, **269**, 383–386.
41 G. Geneste, F. Bouyer and S. Gin, *J. Non-Cryst. Solids*, 2006, **352**, 3147–3152.
42 S. Tonarini, C. Forte, R. Petrini and G. Ferrara, *Geochim. Cosmochim. Acta*, 2003, **67**, 1863–1873.
43 P. Frugier, S. Gin, Y. Minet, T. Chave, B. Bonin, N. Godon, J. E. Lartigue, P. Jollivet, A. Ayral, L. De Windt and G. Santarini, *J. Nucl. Mater.*, 2008, **380**, 8–21.
44 A. J. Spivack and J. M. Edmond, *Geochim. Cosmochim. Acta*, 1987, **51**, 1033–1043.
45 X. Li, H. Y. Li, J. G. Ryan, G. J. Wei, L. Zhang, N. B. Li, X. L. Huang and Y. G. Xu, *Chem. Geol.*, 2019, **505**, 76–85.
46 C. Boschi, A. Dini, G. L. Früh-Green and D. S. Kelley, *Geochim. Cosmochim. Acta*, 2008, **72**, 1801–1823.